Chinese Chemical Letters 37 (2026) 112190

Contents lists available at ScienceDirect

Chinese Chemical Letters

journal homepage: www.elsevier.com/locate/cclet

Three-step cascade artificial light-harvesting system for photooxidation reaction based on cation-pillar[5]arene

Guangping Sun[a,*], Menglian Hu[a], Lujie Wu[a], Danping Zhu[a], Weixuan Ji[a], Yan Sun[a], Menghang Li[a], Jinli Zhu[a], Yanfeng Tang[b], Yong Yao[a,*]

[a] School of Chemistry and Chemical Engineering, Nantong University, Nantong 226019, China
[b] Taizhou University, Taizhou 225300, China

ARTICLE INFO

Article history:
Received 13 September 2025
Revised 15 November 2025
Accepted 26 November 2025
Available online 27 November 2025

Keywords:
Self-assembly
Three-step energy transfer
Artificial light-harvesting
Photooxidation reaction
Cation-pillar[5]arene

ABSTRACT

A three-step cascade artificial light-harvesting system was constructed by the supramolecular assembly of cation-pillar[5]arene (CP5), tetraphenylethene-sulfonate (TPESF), 4,7-di(2-thienyl)-2,1,3-benzothiadiazole (DBT), sulforhodamine 101 (SR101) and chlorin e6 (Ce6). Inspired by the aggregate state in nanoparticles, CP5-TPESF nanoparticles emitted significant blue fluorescence as FRET donors because of TPESF's AIE effect. Due to the donor emission overlapping the acceptors' absorption, a three-step sequential energy transfer process was successfully constructed in CP5-TPESF-DBT-SR101-Ce6 nanoparticles, which achieved the significant energy transfer efficiency of 87 % and antenna effect of 30.8. Benefitting to three-step cascade light-harvesting process and energy transfer to Ce6, Ce6* was excited to release $^1O_2$ in CP5-TPESF-DBT-SR101-Ce6 nanoparticles, which was used as efficient photooxidation catalyst to realize the photooxidation reaction of 4-(methylthio)toluene to 4-(methylsulfinyl)toluene. Notably, the photooxidation yield of CP5-TPESF-DBT-SR101-Ce6 LHS was significantly improved to 89 %, suggesting potential in converting solar energy to chemical energy storage.

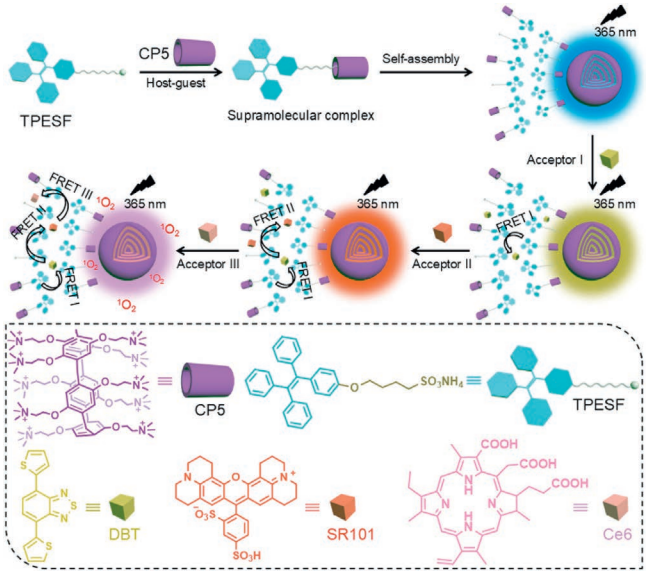
© 2026 Published by Elsevier B.V. on behalf of Chinese Chemical Society and Institute of Materia Medica, Chinese Academy of Medical Sciences.

Natural light-harvesting systems (LHSs) are the energetic and material foundation in living system, which convert sunlight to chemical energy storage by photosynthesis [1–3]. In photosynthesis system, chlorophyll-protein complex structure is highly arranged by supramolecular noncovalent assembly and its absorbed solar energy is sequential cascade transferred to reaction area for energy conversion by fluorescence resonance energy transfer (FRET) [4]. In order to imitate light-harvesting capability, a series of artificial LHSs were constructed and utilized in photo-functional materials [5–13]. Recently, supramolecular assembly strategy had been widely used to construct artificial LHSs due to the higher assembly efficiency and easier synthesis procedure [14–16]. Moreover, benefitting from aggregation-induced emission (AIE) mechanism, AIE donor-based supramolecular artificial LHSs could not only be constructed in water environment, but also output the harvested energy for further application [17–19]. However, most constructed artificial LHSs only focused on one-step or two-step energy transfer process, which were always limited in the wavelength absorption range of sunlight, suggesting a significant lower efficiency compared to natural LHS's broad wavelength absorption [20–22]. Thus, the development of three-step (multi-step) cascade artificial LHSs were necessary and desired to improve the light-harvesting efficiency. So far, only several supramolecular artificial LHSs with three-step energy transfer process have been constructed [23–25]. For example, Liu *et al.* constructed a multi-path cascade artificial LHS based on sulfonatocalix[4]arene, which was utilized for multicolor luminescence with high energy transfer efficiency [23]. Yi *et al.* designed a three-step cascaded artificial LHS based on metallacycles, which could regulate the efficiency by adjusting hydrophilic-hydrophobic interactions [24]. Xing *et al.* developed a three-step sequential energy transfer LHS based on cucurbit[7]uril and sulfobutylether-β-cyclodextrin, which realized the harvested energy for photocatalysis [25]. The construction of the above reported three-step cascade artificial LHSs all relied on neutral metallacycle or anion macrocycle, while cation macrocycle-based three-step cascade artificial LHSs have been rarely reported. It is still a challenge to develop an efficient three-step cascade artificial LHS based on cation macrocycle and facilitate the harvested solar energy conversion to chemical energy storage.

In this work, a three-step cascade artificial LHS based on cation-pillar[5]arene (CP5) and tetraphenylethene-sulfonate (TPESF) was constructed *via* supramolecular strategy. As shown in Scheme 1,

* Corresponding authors.
E-mail addresses: sunguangping1989@ntu.edu.cn (G. Sun), yaoyong1986@ntu.edu.cn (Y. Yao).

https://doi.org/10.1016/j.cclet.2025.112190
1001-8417/© 2026 Published by Elsevier B.V. on behalf of Chinese Chemical Society and Institute of Materia Medica, Chinese Academy of Medical Sciences.



Scheme 1. Schematic illustration of three-step cascade artificial light-harvesting system based on cation-pillar[5]arene.

after host-guest interaction of CP5 and TPESF, CP5-TPESF complex was driven by hydrophilic-hydrophobic interaction and self-assembled into CP5-TPESF nanoparticles, which emitted a significant blue fluorescence under 365 nm irradiation. Due to the blue fluorescence band covering the absorption of 4,7-di(2-thienyl)-2,1,3-benzothiadiazole (DBT), a one-step FRET process could occur in CP5-TPESF-DBT nanoparticles, whose fluorescence color changed to yellow emission. Inspired by this, sulforhodamine 101 (SR101) was used as acceptor II because of its absorption within the fluorescence emission of CP5-TPESF-DBT nanoparticles, facilitating the construction of two-step sequential energy transfer process in CP5-TPESF-DBT-SR101 nanoparticles. Moreover, because the red fluorescence band of CP5-TPESF-DBT-SR101 nanoparticles covered the absorption of chlorin e6 (Ce6), a three-step cascade artificial LHS was realized in CP5-TPESF-DBT-SR101-Ce6 nanoparticles. Notably, benefitting to the three-step sequential energy transfer process and photoactivation of Ce6, CP5-TPESF-DBT-SR101-Ce6 LHS could be used as an aqueous photocatalyst to achieve the photooxidation reaction of 4-(methylthio)toluene, converting the harvested solar energy to chemical energy storage.

CP5 and TPESF were all synthesized by only two-step reaction (Schemes S1 and S2, Figs. S1–S6 in Supporting information) [26–28]. The UV absorption spectra of CP5, TPESF, and CP5-TPESF solution were firstly investigated. As shown in Fig. S7 (Supporting information), after together adding CP5 and TPESF in water, the absorption spectrum of CP5-TPESF solution displayed the significant red shift, revealing host-guest interaction of CP5 and TPESF. Moreover, for amply evaluating the host-guest interaction details in CP5 and TPESF, the sulfonate model guest (SFMG) was substituted for TPESF to explore their interaction details. As shown in Fig. 1, after adding CP5 and SFMG in D_2O, the H_a-H_d peaks of SFMG visibly moved to upfield and their peak shapes split unclearly, but the H_i-H_v peaks of CP5 conversely shifted to downfield, indicating the interaction of CP5 and SFMG. Besides, 2D NOESY spectrum of CP5-SFMG solution further displayed their interaction signals, indicating SFMG had bound in CP5's cavity. ^{1}H NMR titrations of SFMG and CP5 were subsequently explored to investigate the stability of CP5-SFMG complex. Based on SFMG's chemical shift changes, the association constant (K_a) of CP5-SFMG complex was fitted to be 786 ± 89 L/mol, displaying CP5-SFMG complex stable in water (Fig. S8 in Supporting information).

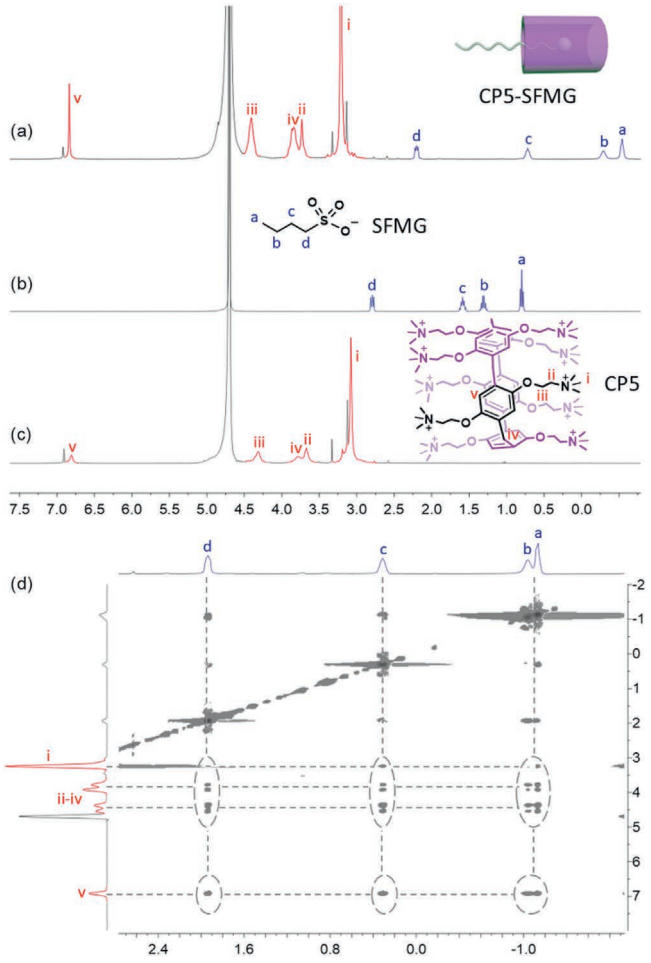


Fig. 1. ^{1}H NMR spectra of (a) CP5-SFMG, (b) SFMG, (c) CP5. (d) 2D NOESY spectrum of CP5-SFMG.

Based on the significant interaction between CP5 and TPESF, a remarkable Tyndall effect phenomenon was observed after preparing CP5-TPESF solution, which illustrated nanoparticles generated in solution. To explore the best molar ratio of CP5 and TPESF for self-assembly into nanoparticles, different molar ratios of CP5 and TPESF solutions were prepared and tested to obtain their UV–vis transmittance spectra (Fig. S9 in Supporting information). According to the transmittance changes at 527 nm, TPESF and CP5 exhibited the best assembly result at 20:2 molar ratio. Moreover, different concentrations solutions of CP5-TPESF at 20:2 molar ratio were prepared to test the critical self-assembly concentration of CP5-TPESF complex. Based on the transmittance changes at 527 nm, CP5-TPESF's critical self-assembly concentration was calculated to be 0.016 mmol/L (Fig. S10 in Supporting information). Notably, after encapsulating DBT, SR101, and Ce6 dyes, the same Tyndall effect phenomena were observed in CP5-TPESF-DBT, CP5-TPESF-DBT-SR101, and CP5-TPESF-DBT-SR101-Ce6 solutions. In order to investigate the size distributions and micromorphology of these nanoparticles, the dynamic light scattering (DLS) and scanning electron microscopy (SEM) experiments of these nanoparticles were carried out, respectively. As shown in Fig. 2, the size distribution of CP5-TPESF nanoparticles was 90–280 nm and its average diameter was 181 nm. The micromorphology of CP5-TPESF nanoparticles displayed a nano-spherical structure, whose diameters coincided with the DLS result. Besides, CP5-TPESF-DBT, CP5-TPESF-DBT-SR101, and CP5-TPESF-DBT-SR101-Ce6 nanoparticles all exhibited narrower distributions, whose average diameters were 170, 178, and 177 nm,

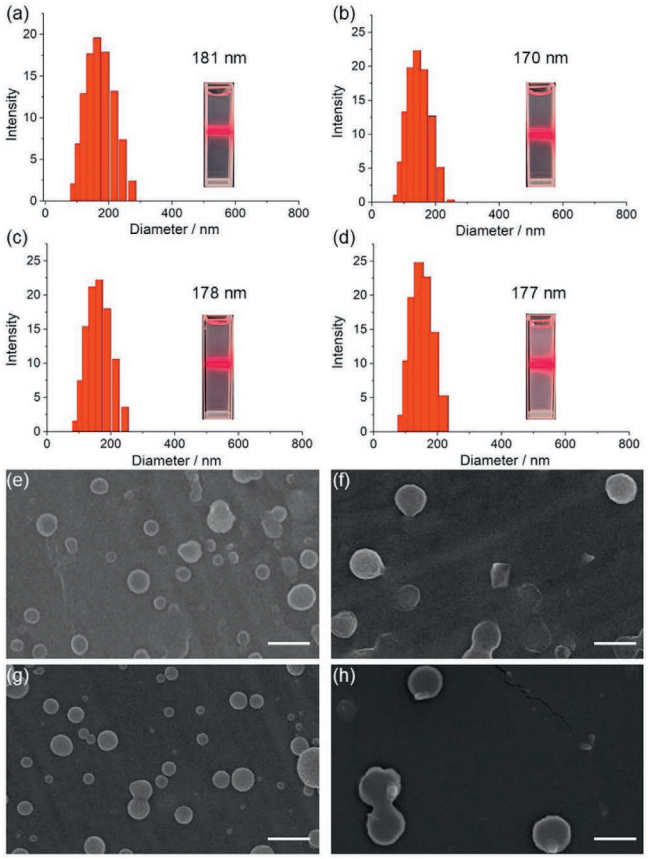


Fig. 2. Size distribution spectra of (a) CP5-TPESF, (b) CP5-TPESF-DBT, (c) CP5-TPESF-DBT-SR101, and (d) CP5-TPESF-DBT-SR101-Ce6 nanoparticles. SEM images of (e) CP5-TPESF, (f) CP5-TPESF-DBT, (g) CP5-TPESF-DBT-SR101, and (h) CP5-TPESF-DBT-SR101-Ce6 nanoparticles. Inset: Tyndall effect photos of nanoparticles solution. Scale bar: 200 nm.

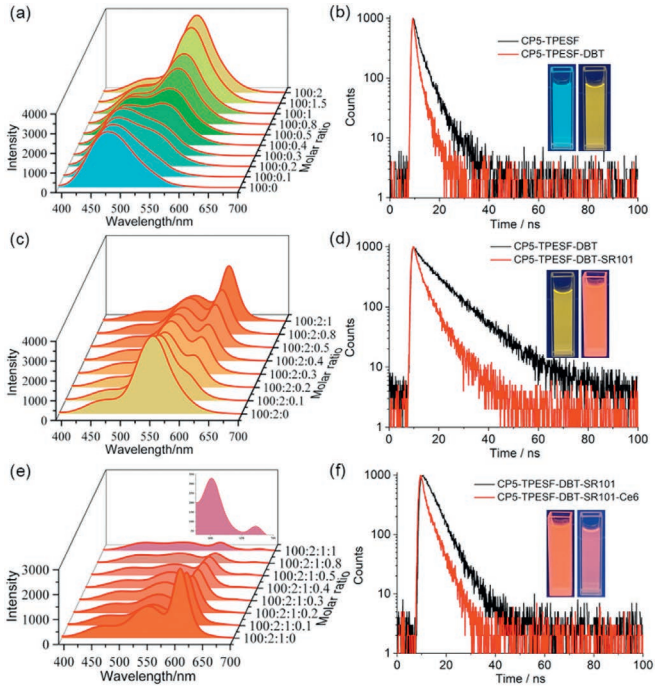


Fig. 3. (a) One-step energy transfer fluorescence spectra and (b) lifetime decay curves of CP5-TPESF-DBT nanoparticles. (c) Two-step energy transfer fluorescence spectra and (d) lifetime decay curves of CP5-TPESF-DBT-SR101 nanoparticles. (e) Three-step energy transfer fluorescence spectra and (f) lifetime decay curves of CP5-TPESF-DBT-SR101-Ce6 nanoparticles. Inset: Fluorescence photos of energy transfer process.

respectively. SEM images of CP5-TPESF-DBT, CP5-TPESF-DBT-SR101, and CP5-TPESF-DBT-SR101-Ce6 nanoparticles displayed the same spherical morphology and particle distribution. Subsequently, zeta potential experiments were tested to evaluate the stability of CP5-TPESF, CP5-TPESF-DBT, CP5-TPESF-DBT-SR101, and CP5-TPESF-DBT-SR101-Ce6 nanoparticles in water (Tables S1–S3 and Fig. S11 in Supporting information). Benefitting to the encapsulation of DBT, SR101, and Ce6, the zeta potentials of supramolecular nanoparticles were significantly increased from 24.9 mV in CP5-TPESF nanoparticles to 41.5 mV in CP5-TPESF-DBT-SR101-Ce6 nanoparticles, indicating CP5-TPESF-DBT-SR101-Ce6 nanoparticles more stable for light-harvesting and energy transfer in aqueous solution (Fig. S27 in Supporting information).

Due to the AIE property in TPESF, the aggregated TPESF in CP5-TPESF nanoparticles could emit a significant blue fluorescence and conduct as donor for constructing FRET process. DBT was considered as acceptor I to realize the first step energy transfer process because of CP5-TPESF's blue fluorescence band fully covering DBT's absorption (Fig. S12 in Supporting information). As shown in Figs. 3a and b, after loading DBT, the blue fluorescence intensity of CP5-TPESF was immediately weakened, but the emission intensity of DBT appeared a rapid increase and the fluorescence color of CP5-TPESF-DBT nanoparticles significantly changed to yellow, confirming the first step energy transfer in CP5-TPESF-DBT. Besides, the fluorescence lifetime decay change of donor (CP5-TPESF) was explored to reveal the light-harvesting characteristic. According to the fitting calculation of CP5-TPESF's decay curve, the τ_1 and τ_2 of CP5-TPESF nanoparticles were computed to be 1.32 ns and 4.36 ns (Fig. S15 in Supporting information). While the τ_1 and τ_2 of CP5-TPESF-DBT nanoparticles were computed to be 0.91 ns and 2.88 ns after TPESF's energy transferred to DBT, whose τ exhibited a significant attenuation from 3.60 ns to 1.92 ns, confirming the successful construction of one-step artificial light-harvesting process in CP5-TPESF-DBT nanoparticles (Fig. S16 in Supporting information). The energy transfer efficiency and antenna effect of CP5-TPESF-DBT nanoparticles were calculated to be 78 % and 78.8, suggesting CP5-TPESF's excellent light-harvesting antenna ability (Figs. S21 and S24 in Supporting information).

Moreover, as DBT's emission part in CP5-TPESF-DBT totally covered SR101's absorption, SR101 was utilized as acceptor II to construct two-step sequential artificial LHS (Fig. S13 in Supporting information). When SR101 was loaded in CP5-TPESF-DBT nanoparticles, DBT's emission intensity significantly decreased (Fig. 3c). But SR101's emission intensity rapidly increased and the fluorescence color of CP5-TPESF-DBT-SR101 nanoparticles solution turned into red, attributing to the second step energy transfer from SR101 to DBT. The τ_1, τ_2 were observed to decrease from 3.97 ns, 11.30 ns of CP5-TPESF-DBT nanoparticles to 1.89 ns, 6.09 ns of CP5-TPESF-DBT-SR101 nanoparticles, confirming the assembly of two-step sequential artificial LHS (Fig. 3d, Figs. S17 and S18 in Supporting information). The energy transfer efficiency and antenna effect of CP5-TPESF-DBT-SR101 nanoparticles were calculated to be 67 % and 17.5 (Figs. S22 and S25 in Supporting information). Furthermore, considering the spectra coverage between Ce6's absorption and the emission of CP5-TPESF-DBT-SR101 nanoparticles, Ce6 was chosen as acceptor III to construct the third step energy transfer (Fig. S14 in Supporting information). After Ce6 loaded in CP5-TPESF-DBT-SR101 nanoparticles, the intensity of SR101's emission appeared significant attenuation and the emission of Ce6 was gradually observed in CP5-TPESF-DBT-SR101-Ce6 nanoparticles, whose fluorescence color turned to pink, indicating the successful third step energy transfer (Figs. 3e and f). The τ of SR101's emis-

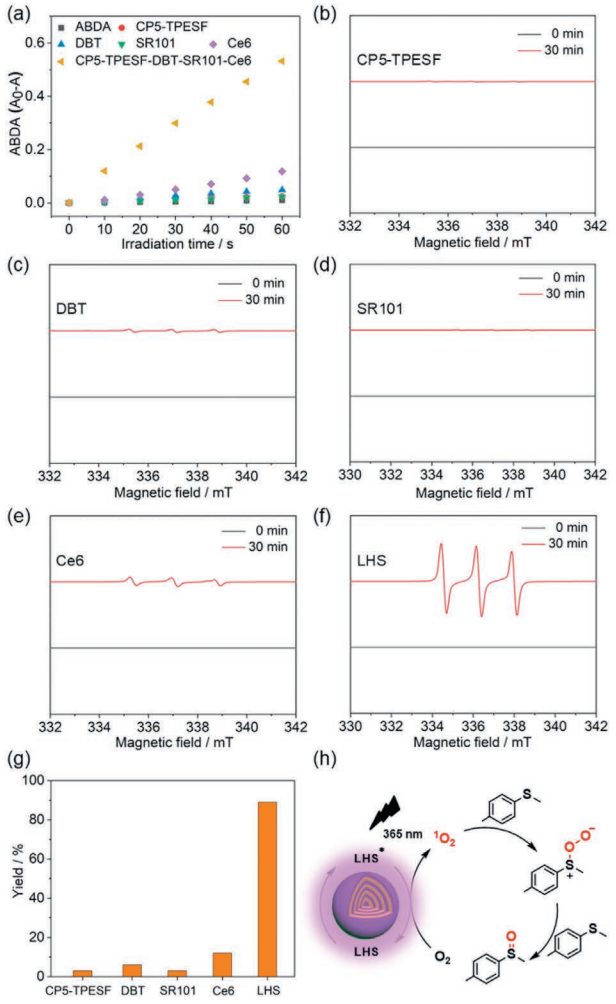


Fig. 4. (a) Absorption quench spectra of ABDA, CP5-TPESF+ABDA, DBT+ABDA, SR101+ABDA, Ce6+ABDA, and CP5-TPESF-DBT-SR101-Ce6+ABDA solutions at 375 nm under 365 nm irradiation. EPR spectra of (b) CP5-TPESF, (c) DBT, (d) SR101, (e) Ce6, and (f) CP5-TPESF-DBT-SR101-Ce6 solutions with TEMP as $^1O_2$ capturing agent under 365 nm irradiation for 30 min. (g) The photooxidation yields. (h) The proposed $^1O_2$ photooxidation mechanism of 4-(methylthio)toluene to 4-(methylsulfinyl)toluene.

sion was decayed from 4.83 ns in CP5-TPESF-DBT-SR101 nanoparticles to 3.56 ns in CP5-TPESF-DBT-SR101-Ce6 nanoparticles, further confirming the construction of three-step artificial LHS (Figs. S19 and S20 in Supporting information). The energy transfer efficiency and antenna effect of CP5-TPESF-DBT-SR101-Ce6 nanoparticles were calculated to be 87 % and 30.8, whose light-harvesting performance exhibited potential in solar energy conversion (Figs. S23 and S26 in Supporting information).

After achieving three-step artificial light-harvesting process, the harvested solar energy was attempted to catalyze chemical reaction and convert into chemical energy storage. The sulfoxides were important intermediates in pharmaceutical synthesis and chemical industry manufacture, which were usually synthesized by the oxidation of sulfides [29]. Inspired by the excellent light-harvesting ability, the singlet oxygen ($^1O_2$) production of CP5-TPESF-DBT-SR101-Ce6 nanoparticles was initially evaluated by 9,10-anthracenediylbis(methylene)dimalonic acid (ABDA) indicator based on its absorbance quench at 375 nm (Figs. S28 and S29 in Supporting information) [30–32]. As shown in Fig. 4a, no significant absorbance quench was observed in CP5-TPESF, DBT, SR101, and Ce6 solutions, indicating the weak ability of $^1O_2$ production. Moreover, electron paramagnetic resonance (EPR) measurements were directly utilized to detect the $^1O_2$ production by 2,2,6,6-tetramethylpiperidine (TEMP) [33,34]. The EPR spectra of CP5-TPESF, DBT, SR101, and Ce6 solutions also displayed weak signals, corresponding to the above ABDA results (Figs. 4b–e). However, compared to the limited $^1O_2$ production of free donor and acceptors, the significant absorbance quench and triple peak of $^1O_2$ were observed in CP5-TPESF-DBT-SR101-Ce6 solution, confirming more energy transferred to activate Ce6 for $^1O_2$ production by three-step artificial light-harvesting process (Figs. 4a and f). Because $^1O_2$ is a green oxidant for the photooxidation reaction, CP5-TPESF-DBT-SR101-Ce6 LHS was utilized as photocatalyst to catalyze the photooxidation reaction of 4-(methylthio)toluene to 4-(methylsulfinyl)toluene, mimicking the solar energy storage of natural LHS (Figs. 4g and h, Scheme S3 in Supporting information) [35]. Notably, no significant oxidation yields were observed in CP5-TPESF, DBT, SR101, and Ce6 solutions due to the poor $^1O_2$ production ability. But the yield of CP5-TPESF-DBT-SR101-Ce6 LHS was significantly improved to 89 %, which was attributed to three-step energy transfer process to generate more excited Ce6 for $^1O_2$ production. Besides, a series of photooxidation products with different substituent groups were also obtained, which significantly demonstrated the wide applicability of this artificial LHS system, suggesting CP5-TPESF-DBT-SR101-Ce6 artificial LHS potential in solar energy storage and utilization (Figs. S30–S38 in Supporting information).

In summary, we have constructed a three-step cascade artificial light-harvesting system based on cation-pillar[5]arene (CP5) and tetraphenylethene-sulfonate (TPESF), which self-assembled into CP5-TPESF nanoparticles as energy donors. Due to the excellent spectra overlap of donor emission and acceptor absorption in energy transfer process, 4,7-di(2-thienyl)-2,1,3-benzothiadiazole (DBT), sulforhodamine 101 (SR101) and chlorin e6 (Ce6) were utilized as FRET acceptors to construct CP5-TPESF-DBT-SR101-Ce6 three-step sequential energy transfer process, which achieved significant energy transfer efficiency of 87 % and antenna effect of 30.8. Notably, after sequential energy transfer, more Ce6* was excited in CP5-TPESF-DBT-SR101-Ce6 LHS, which produced significant $^1O_2$ under 365 nm irradiation. Inspired by the oxidation ability of $^1O_2$, CP5-TPESF-DBT-SR101-Ce6 LHS was utilized as photocatalyst for the photooxidation reaction of 4-(methylthio)toluene to 4-(methylsulfinyl)toluene, whose yield was significantly improved to 89 %, suggesting potential in mimicking the energy conversion process of natural LHS.

CRediT authorship contribution statement

Guangping Sun: Writing – review & editing, Writing – original draft, Investigation, Funding acquisition, Conceptualization. **Menglian Hu:** Writing – original draft, Investigation, Formal analysis, Data curation. **Lujie Wu:** Investigation. **Danping Zhu:** Investigation. **Weixuan Ji:** Investigation. **Yan Sun:** Investigation. **Menghang Li:** Investigation. **Jinli Zhu:** Conceptualization. **Yanfeng Tang:** Conceptualization. **Yong Yao:** Writing – review & editing, Writing – original draft, Investigation, Conceptualization.

Declaration of competing interest

The authors declare that they have no known competing financial interests or personal relationships that could have appeared to influence the work reported in this paper.

Acknowledgments

This work was supported by the National Natural Science Foundation of China (No. 22401160), the Natural Science Foundation of Jiangsu Province (No. BK20220601), the Open Project of State Key

Laboratory of Synergistic Chem-Bio Synthesis (No. sklscbs202515), and the Training Programs of Innovation for Undergraduates (No. 2025078). We are very grateful to the Nantong University Analysis & Testing Center for its support in testing.

Supplementary materials

Supplementary material associated with this article can be found, in the online version, at doi:10.1016/j.cclet.2025.112190.

References

[1] P. Qian, C.A. Siebert, P. Wang, D.P. Canniffe, C.N. Hunter, Nature 556 (2018) 203–208.
[2] X. Pan, J. Ma, X. Su, et al., Science 360 (2018) 1109–1113.
[3] T.K. Baikie, L.T. Wey, J.M. Lawrence, et al., Nature 615 (2023) 836–840.
[4] T. Mirkovic, E.E. Ostroumov, J.M. Anna, et al., Chem. Rev. 117 (2017) 249–293.
[5] X. Zhou, X. Bai, F. Shang, et al., Nat. Commun. 15 (2024) 4787.
[6] Q. Duan, Q. Zhang, J. Zhang, et al., Chin. Chem. Lett. 36 (2025) 111421.
[7] B. Mu, X. Hao, X. Luo, et al., Nat. Commun. 15 (2024) 903.
[8] R. Zhang, X. Tian, M. Zuo, et al., Adv. Sci. 12 (2025) 2504993.
[9] L. Chu, Q. Liu, R. Zhang, K. Wang, X.Y. Hu, Green Synth. Catal. (2025), doi:10.1016/j.gresc.2025.03.012.
[10] Q. Ning, Y. Zhang, H. Sun, et al., Chin. Chem. Lett. 36 (2025) 111133.
[11] L. Zhou, Y. Zhou, L. Fang, et al., Chin. Chem. Lett. 35 (2024) 109509.
[12] J.C. Yang, K. Chen, G.L. Zhang, et al., Chem. Sci. 16 (2025) 4741–4748.
[13] R. Cen, Y.Y. Tang, L.X. Chen, Z. Tao, X. Xiao, Chin. Chem. Lett. 36 (2025) 109744.
[14] Y. Bi, R. Zhang, K. Niu, et al., Chin. Chem. Lett. 36 (2025) 110311.
[15] Q. Zhang, X. Dang, F. Cui, T. Xiao, Chem. Commun. 60 (2024) 10064–10079.
[16] Y.X. Hu, W.J. Li, P.P. Jia, et al., Adv. Optical Mater. 8 (2020) 2000265.
[17] M. Hao, G. Sun, M. Zuo, et al., Angew. Chem. Int. Ed. 59 (2020) 10095–10100.
[18] G. Sun, M. Li, L. Cai, et al., Chem. Commun. 60 (2024) 1412–1415.
[19] G. Sun, M. Li, J. Li, et al., Chem. Commun. 61 (2025) 6360–6363.
[20] C. Li, Q. Liu, S. Tao, Nat. Commun. 13 (2022) 6034.
[21] Y. Li, C. Xia, R. Tian, et al., ACS Nano 16 (2022) 8012–8021.
[22] K.X. Teng, Z.P. An, L.Y. Niu, Q.Z. Yang, ACS Mater. Lett. 6 (2024) 290–297.
[23] W.W. Xu, Y.X. Qin, X.Y. Yu, et al., Chin. Chem. Lett. 36 (2025) 111068.
[24] D. Zhang, M. Li, B. Jiang, et al., J. Colloid Interface Sci. 652 (2023) 1494–1502.
[25] R.Z. Zhang, Y.S. Bi, K.K. Niu, et al., Adv. Optical Mater. 13 (2025) 2402112.
[26] Y. Yang, J. Yang, Y. Du, et al., ACS Omega 4 (2019) 17741–17751.
[27] X.Y. Hu, X. Liu, W. Zhang, et al., Chem. Mater. 28 (2016) 3778–3788.
[28] D.G. Khandare, H. Joshi, M. Banerjee, M.S. Majik, A. Chatterjee, Anal. Chem. 87 (2015) 10871–10877.
[29] Y. Zhang, Y. Su, L. Liu, B. Chen, Chem. Commun. 61 (2025) 7795–7798.
[30] J.Y. Liu, R.Z. Zhang, N. Han, H. Liu, L.B. Xing, J. Mater. Chem. A 13 (2025) 13789–13796.
[31] Z.H. Zhu, Y.L. Li, H.L. Wang, et al., J. Colloid Interface Sci. 685 (2025) 458–467.
[32] H. Sun, S. Li, Q. Liu, et al., Chin. Chem. Lett. 36 (2025) 109999.
[33] J.H. Wu, F. Chen, T.H. Yang, H.Q. Yu, Proc. Natl. Acad. Sci. U. S. A. 120 (2023) e2305706120.
[34] Y. Tian, Y. Li, Y. Li, et al., Sep. Purif. Technol. 355 (2025) 129564.
[35] M.X. Liu, X.L. Su, P. Chen, et al., Chin. Chem. Lett. 37 (2026) 111516.